



1 **Comparison of Modified Bligh-Dyer and Ultrasonic**
2 **Organic Solvent Methods for GDGT Extraction from**
3 **Surface Sediments of Lakes with Different Salinities**

4 Rui Miao^{1,2}, Ning Shi^{1,2}, Zenghao Zhao¹, Hu Liu^{3,4}, Xiangzhong Li⁵, Huanye Wang¹

5 ¹State Key Laboratory of Loess Science, Institute of Earth Environment, Chinese Academy of Sciences,
6 Xi'an 710061, China

7 ²University of Chinese Academy of Sciences, Beijing 100049, China.

8 ³School of Water and Environment, Chang'an University, Xi'an 710064, China.

9 ⁴Key Laboratory of Subsurface Hydrology and Ecological Effect in Arid Region of the Ministry of
10 Education, Chang'an University, Xi'an 710064, China.

11 ⁵Yunnan Key Laboratory of Earth System Science, School of Earth Science, Yunnan University,
12 Kunming 650500, China.

13 *Correspondence to:* Huanye Wang (wanghy@ieecas.cn)

14 **Abstract.** Accurately quantifying core lipid (CL) and intact polar lipid (IPL) GDGTs is essential for
15 investigating the sources of GDGTs and their responses to climatic and environmental changes in
16 lacustrine systems. However, systematic comparisons of the performance of different methods for
17 extracting GDGTs (both abundance and distribution) from lake sediments remain limited. In this study,
18 we compared two ultrasonic organic solvent extraction methods, including a stepwise gradient extraction
19 with dichloromethane/methanol (DCM/MeOH) solvent mixtures of different polarities and a single
20 solvent extraction with DCM:MeOH (9:1, v:v), and two modified Bligh-Dyer (BD) methods (phosphate
21 buffer; trichloroacetic acid) for extracting CL-GDGTs and IPL-GDGTs from saline and freshwater lake
22 sediments. The results showed that, for CL-GDGTs, stepwise gradient extraction yielded the highest
23 recovery, whereas no significant differences were observed in the CL-derived GDGTs proxies among
24 the different extraction methods. For IPL-GDGTs, the BD (phosphate buffer) method achieved the
25 highest recovery for isoprenoid GDGTs (isoGDGTs), while stepwise gradient extraction was most
26 effective for extracting branched GDGTs (brGDGTs) and archaeol from saline lake sediments. Moreover,
27 the consistently lower relative abundance of crenarchaeol to other isoGDGTs in CLs than in IPLs for all
28 methods suggests that crenarchaeol is primarily produced in the lake water column, whereas other
29 isoGDGTs have a relatively greater autochthonous production within the sediments or at the water-
30 sediment interface. In saline lake sediments, we also observed higher relative abundance of ≥ 7 -methyl



31 brGDGTs and tetramethylated brGDGTs in IPLs than in CLs, indicating that their source bacteria are
32 active at the water-sediment interface or in the sediments of saline lakes. These findings will provide
33 insights for the quantitative analysis of GDGTs in lake sediments and for the study of their sources in
34 lacustrine environments.

35 **1 Introduction**

36 Glycerol Dialkyl Glycerol Tetraethers (GDGTs) are unique lipid components of archaeal and
37 bacterial cell membranes. Owing to their stable molecular structures and sensitive responses to
38 environmental changes, they have become important biomarkers in the field of paleoclimate
39 reconstruction (e.g., Hopmans et al., 2004; Weijers et al., 2007; Blaga et al., 2009; Turich and Freeman,
40 2011; Zhang et al., 2011; De Jonge et al., 2014; Wang et al., 2014; De Jonge et al., 2015; Wang et al.,
41 2021). Environmental proxies based on GDGTs have been widely applied in paleoclimate and
42 paleoenvironmental studies across various geological archives, including marine sediments, lakes, peat,
43 and loess (e.g., Schouten et al., 2013; Inglis et al., 2022; Rezanka et al., 2023).

44 In living microbial cells, GDGTs primarily exist as intact polar lipids (IPL), whose molecular
45 structure consists of a core tetraether skeleton with polar head groups attached at both ends. These polar
46 head groups mainly include sugar-based head groups such as monohexose (MH), dihexose (DH),
47 phosphohexose (PH), and hexose-phosphohexose (HPH) (Sturt et al., 2004; Schouten et al., 2008; Pitcher
48 et al., 2011; Zheng et al., 2025), as well as phospholipid head groups (Sturt et al., 2004; Pitcher et al.,
49 2009; Zheng et al., 2025). Following cell death, some polar head groups are removed through microbial
50 degradation or during early diagenesis, gradually forming stable and well-preserved core lipid (CL)
51 GDGTs. This process results in the common coexistence of both IPL-GDGTs and CL-GDGTs in natural
52 samples.

53 Lake sediments serve as important geological archives for paleoenvironmental research. Although
54 current paleoclimate reconstructions primarily rely on GDGT-based proxies derived from the distribution
55 of CL-GDGTs, an increasing number of studies find that the production, transformation rates, and
56 preservation efficiency of GDGTs significantly influence the accuracy of the resulting proxies. Therefore,
57 investigating IPL-GDGTs in lakes is fundamental to understanding the response mechanisms of GDGTs



58 to environmental parameters. Previous studies have revealed that the production of IPL-GDGTs in the
59 water column of both shallow and deep lakes exhibits pronounced seasonal variations (Buckles et al.,
60 2014; Qian et al., 2019; van Bree et al., 2020; Baxter et al., 2021). Additionally, the primary productivity
61 of GDGTs varies across different water depths, which can ultimately lead to biases in the “temperature
62 signal” recorded in surface sediments (Weber et al., 2018; Meegan Kumar et al., 2019; Baxter et al.,
63 2021). In addition to the water column, GDGTs can also be produced within lake surface sediments,
64 introducing further biases into the proxies and thereby complicating the interpretation and application of
65 these environmental proxies (Tierney et al., 2012; Qian et al., 2019; Raberg et al., 2022). Consequently,
66 establishing an analytical method that enables the accurate quantification of both CL-GDGTs and IPL-
67 GDGTs is essential for reducing quantification errors, improving data accuracy, distinguishing between
68 living and sedimentary signals, and providing a more robust chemical foundation for paleoclimate
69 reconstruction and microbial ecology research.

70 Currently, two major strategies are employed for the analysis of IPL-GDGTs. The first is the direct
71 analysis method, which involves the direct determination of IPL-GDGTs in total lipid extracts (TLEs,
72 including both CL and IPL fractions) using high-performance liquid chromatography coupled with
73 electrospray ionization mass spectrometry (HPLC-ESI-MS) (e.g., Sturt et al., 2004; Huguet et al., 2010b;
74 Van Mooy and Fredricks, 2010; Chen et al., 2016; Horai et al., 2019). The second is the indirect analysis
75 method, which typically employs normal-phase high-performance liquid chromatography coupled with
76 atmospheric pressure chemical ionization mass spectrometry (HPLC-APCI-MS) to measure CL-GDGTs
77 derived from the acid hydrolysis of IPL-GDGTs, with the measured CL-GDGTs representing the IPL-
78 GDGT concentration. The indirect method can be further divided into two approaches. One approach
79 involves separating CL-GDGTs from IPL-GDGTs in TLEs using a silica gel column, followed by
80 hydrolysis of the IPL-GDGT fraction and quantification of the resulting CL-GDGTs (e.g., Pitcher et al.,
81 2009; Ingalls et al., 2012; Lengger et al., 2012; Zhu et al., 2013). The second approach employs a
82 “subtraction method”, in which the TLE is split into two aliquots, one aliquot is directly analyzed for its
83 original CL-GDGT concentration, while the other aliquot is subjected to acid hydrolysis to convert IPL-
84 GDGTs into CL-GDGTs, and the total CL-GDGTs (i.e., the sum of IPL-GDGTs and CL-GDGTs) is then
85 measured. The IPL-GDGT concentration is calculated as the difference between the two measurements



86 (e.g., Huguet et al., 2010b; Lengger et al., 2012). Due to variations in the ionization efficiencies of
87 different IPL-GDGTs in mass spectrometry, direct quantification of IPL-GDGTs is challenging (Zink et
88 al., 2008). In contrast, the indirect method circumvents this difficulty by uniformly quantifying CL-
89 GDGTs, and is therefore the most commonly employed approach (Bijl et al., 2025; Li et al., 2025).

90 For the extraction of GDGTs, various methods can be employed to extract TLEs from environmental
91 or culture samples. These include ultrasonic organic solvent extraction (e.g., Schouten et al., 2007;
92 Huguet et al., 2010b; Ingalls et al., 2012; Wang et al., 2017; Weber et al., 2017), the modified Bligh-Dyer
93 (BD) method (e.g., Huguet et al., 2010b; Lengger et al., 2012; Buckles et al., 2014; Wang et al., 2017;
94 Weber et al., 2017; Qian et al., 2019; van Bree et al., 2020; Raberg et al., 2022), Soxhlet extraction (e.g.,
95 Schouten et al., 2007; Huguet et al., 2010b; Lengger et al., 2012), accelerated solvent extraction (ASE)
96 (e.g., Schouten et al., 2007; Huguet et al., 2010b; Lengger et al., 2012), and microwave-assisted
97 extraction (MAE) (e.g., Escala et al., 2007; Huguet et al., 2010b; Pearson et al., 2011), among others.
98 However, different extraction methods exhibit varying efficiencies for the extraction of CL-GDGTs and
99 IPL-GDGTs (Bijl et al., 2025; Li et al., 2025). For CL-GDGTs, previous studies have shown that the
100 GDGT-derived indices obtained using different extraction methods are consistent (Schouten et al., 2007;
101 Wang et al., 2017); therefore, the choice of extraction method generally does not affect the application
102 of CL-GDGT-based proxies. Nevertheless, several studies have demonstrated that extraction efficiencies
103 for IPL-GDGTs vary significantly among different methods. Huguet et al. (2010b) compared the BD
104 method, ultrasonication, Soxhlet extraction, ASE, and MAE, and found that Soxhlet extraction yielded
105 the highest the highest recovery of total IPL-GDGTs from cultured samples and bay suspended
106 particulate matter (SPM). Subsequently, however, Lengger et al. (2012) pointed out that different
107 methods exhibit varying extraction efficiencies for GDGTs containing MH, DH, and HPH head groups;
108 notably, the extraction efficiencies of Soxhlet extraction and ASE for HPH-crenarchaeol were
109 significantly lower than that of the BD method, potentially due to the degradation of IPL-GDGTs under
110 high-temperature conditions or adsorption of IPL-GDGTs to extraction vessels. Wang et al. (2017)
111 observed that, for lake sediment and soil samples, ultrasonic solvent extraction recovered more CL-
112 GDGTs than the BD method, whereas the BD method yielded more IPL-GDGTs. Weber et al. (2017)
113 compared the efficiencies of ultrasonication and the modified BD method for extracting IPL-GDGTs



114 from lake filter samples, finding that although the BD method achieved higher extraction rates,
115 substantial amounts of IPL-brGDGTs were lost in the aqueous phase (particularly in phosphate buffer)
116 and in the solid residue. More recently, Evans et al. (2022) found that repeated freeze-thaw cycles prior
117 to extraction facilitate cell membrane disruption, and that certain chemical detergents, such as
118 cetyltrimethylammonium bromide (CTAB), can significantly improve IPL extraction efficiencies from
119 archaeal pure cultures. In summary, for highly polar and thermally unstable IPL-GDGTs, extraction
120 techniques involving high-temperature conditions may not be advisable. Although some emerging
121 extraction methods offer high IPL-GDGT recoveries, they involve complex and time-consuming
122 procedures that require further optimization or validation across a wide range of natural samples.
123 Consequently, the BD method and ultrasonication remain the most widely used approaches for IPL-
124 GDGT extraction (Bijl et al., 2025).

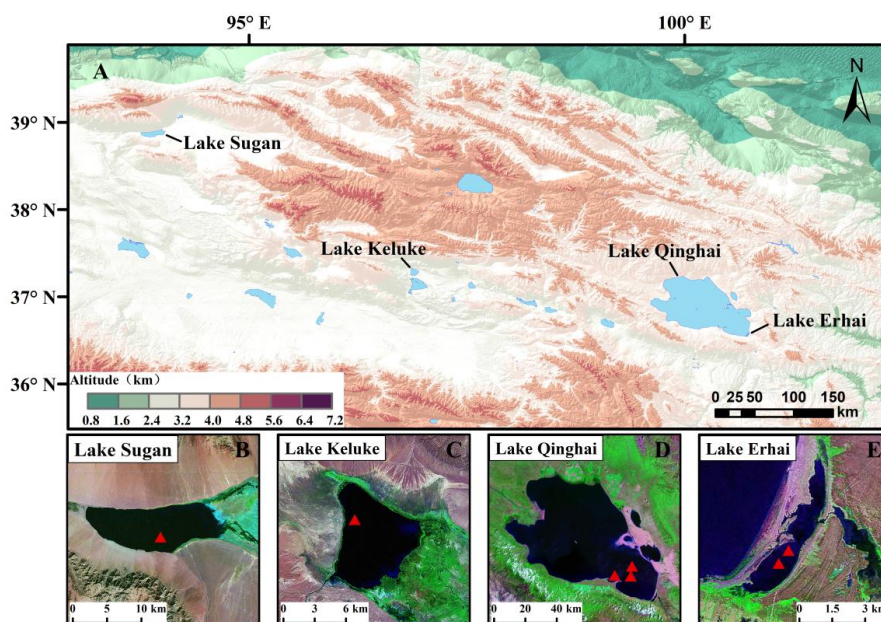
125 As noted above, existing comparative studies on IPL-GDGT extraction methods have
126 predominantly focused on SPM from water columns or microbial culture samples, whereas systematic
127 evaluations of IPL-GDGT (including both iso- and brGDGT) extraction from lake sediments remain
128 limited. Given that sediments and SPM differ in matrix composition, particle structure, and lipid
129 occurrence states, their extraction behaviors may also differ, potentially affecting the accuracy of
130 quantitative results and subsequent environmental interpretations. In this study, we compared the
131 performance of 4 methods for both extracting isoGDGTs and brGDGTs in surface sediments of 4 lakes
132 (including both saline and freshwater lakes) on the Tibetan Plateau. The methods used for comparison
133 include two modified Bligh-Dyer (BD) methods (phosphate buffer (P-buffer) and trichloroacetic acid
134 (TCA)), stepwise gradient extraction with dichloromethane/methanol (DCM/MeOH) solvent mixtures
135 of different polarities (MeOH, MeOH:DCM (1:1, v:v), and DCM), and single solvent extraction with
136 MeOH:DCM (9:1, v:v). Our aim was to provide a basis for selecting appropriate analytical methods for
137 studying CL-GDGTs and IPL-GDGTs for lake sediments. Furthermore, based on these comparisons,
138 differences in distributions of CL-GDGTs and IPL-GDGTs were examined to elucidate potential sources
139 of GDGTs in lacustrine systems.



140 **2 Materials and methods**

141 **2.1 Study Area and Sample Collection**

142 In this study, surface sediment samples were collected from four lakes in the northeastern Tibetan
143 Plateau, including two saline lakes (Qinghai Lake and Sugan Lake) and two freshwater lakes (Keluke
144 Lake and Erhai) (Fig. 1A). Qinghai Lake ($36^{\circ}32' - 37^{\circ}15' \text{ N}$, $99^{\circ}36' - 100^{\circ}47' \text{ E}$) is the largest inland
145 brackish lake in China, with a total dissolved solids (TDS) concentration of approximately 15 g/L, an
146 average water depth of 17.9 m, and a lake water pH of approximately 9.1 (Wang and Dou, 1998). Sugan
147 Lake ($38^{\circ}50' - 38^{\circ}54' \text{ N}$, $93^{\circ}45' - 94^{\circ}00' \text{ E}$) is a sodium sulfate subtype brackish lake with a TDS
148 concentration of approximately 32 g/L, an average water depth of 2.8 m, and a lake water pH of
149 approximately 8.9 (Wang and Dou, 1998). Keluke Lake ($37^{\circ}14' - 37^{\circ}20' \text{ N}$, $96^{\circ}51' - 96^{\circ}57' \text{ E}$) is a sodium
150 sulfate subtype freshwater lake with a TDS concentration below 1 g/L, an average water depth of 2.9 m,
151 and a lake water pH of approximately 8.0 (Wang and Dou, 1998). Erhai is a small freshwater lake formed
152 after the water level decline of Qinghai Lake, located in the southeastern part of Qinghai Lake, with an
153 average water depth of approximately 1.5 m, a pH of approximately 9.0, and a TDS concentration of
154 approximately 1.2 g/L (Lanzhou Institute of Geology, Chinese Academy of Sciences et al., 1979).



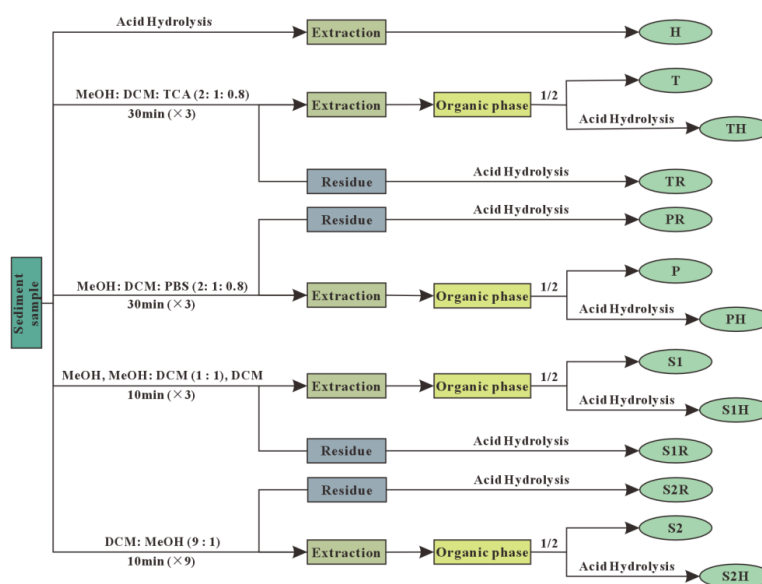
155
156 **Figure 1. Location of the study lakes (A) and sampling sites in Sugan Lake (B), Keluke Lake (C), Qinghai**
157 **Lake (D), and Erhai Lake (E)**



158 Three surface sediment samples from Qinghai Lake were collected in 2021, with sampling site
159 coordinates and corresponding water depths as follows: 100.432672 °E, 36.682831 °N (water depth: 23
160 m), 100.554561 °E, 36.739211 °N (water depth: 27 m), and 100.549753 °E, 36.682936 °N (water depth:
161 28 m) (Fig. 1D). Two surface sediment samples from Erhai were collected in 2019, with coordinates of
162 100.7216 °E, 36.55535 °N (water depth: 3 m) and 100.7267 °E, 36.56064 °N (water depth: 3 m) (Fig.
163 1E). The surface sediment sample from Keluke Lake was collected in 2023 at coordinates 96.873236 °E,
164 37.300164 °N, with a water depth of 6 m (Fig. 1C). The surface sediment sample from Sugan Lake was
165 also collected in 2023 at coordinates 93.890912 °E, 38.854362 °N, with a water depth of 8 m (Fig. 1B).

166 **2.2 Lipid extraction and fractionation**

167 All sediment samples were freeze-dried and ground to homogeneity. The three samples from
168 Qinghai Lake and the two samples from Erhai were each combined into one composite sample, resulting
169 in four lake sediment samples (SG, QH, EH, and KLK). Each sample was divided equally into five
170 aliquots. Among these, two aliquots were extracted using two modified Bligh-Dyer methods, two
171 aliquots were extracted using two ultrasonic extraction methods, and the remaining aliquot was directly
172 subjected to acid hydrolysis for the determination of total GDGTs (Fig. 2). All extractions were
173 performed in polytetrafluoroethylene (PTFE) centrifuge tubes to minimize potential losses of IPL-
174 GDGTs due to adsorption onto glass surfaces (Pitcher et al., 2009).



175

176

Figure 2. Flowchart of the pretreatment procedure for GDGT quantification

177

178

179

180

181

182

183

184

185

186

187

188

189

190

191

192

The modified BD methods were based on the original protocol described by Bligh and Dyer (1959), with the chloroform/methanol (CHCl₃/MeOH) system replaced by the less toxic DCM/MeOH system. P-buffer (White et al., 1979) and TCA aqueous solution (Nishihara and Koga, 1987) were used as the primary solvents for tetraether lipid extraction. Specifically, appropriate volumes of MeOH:DCM:0.1 M P-buffer (2:1:0.8, v:v; pH 7.4) and MeOH:DCM:5 % TCA (2:1:0.8, v:v:v) were added to two aliquots, respectively. Ultrasonic extraction was performed three times, each for 30 min, with an intermediate shaking step during each extraction. After each extraction, the mixture was centrifuged, and the supernatant was collected. The supernatants from the three extractions were combined. To the combined supernatant, additional DCM and P-buffer or TCA were added to adjust the final ratio to 1:1:0.9 (v:v:v) (MeOH:DCM:P-buffer/TCA). After thorough mixing, the mixture was allowed to separate into phases, and the DCM organic phase was collected. The aqueous phase was re-extracted twice with DCM. The organic phases from the three extractions were combined.

For the two aliquots subjected to ultrasonic extraction, different solvent mixtures of MeOH and DCM were used. One aliquot was subjected to three cycles of sequential extraction with MeOH, DCM:MeOH (1:1, v:v), and DCM, each extraction by ultrasonication for 10 min, for a total of 9 extractions. The other aliquot was extracted ultrasonically with DCM:MeOH (9:1, v:v) for nine cycles,



193 each lasting 10 min. The organic phases from the nine cycles were combined for each aliquot.

194 IPL-GDGTs were quantified indirectly using the “subtraction method”, in which the removal of
195 polar head groups via acid hydrolysis yields a difference in GDGT concentration that represents the IPL-
196 GDGT concentration (Pitcher et al., 2009). Specifically, the combined organic phase from each extraction
197 method was spiked with an appropriate amount of C₄₆ GTGT internal standard and then divided into two
198 equal portions. One portion was dried under N₂, redissolved in *n*-hexane, and filtered through a 0.22 μm
199 syringe filter prior to analysis; the GDGTs measured in this portion correspond to CL-GDGTs. The other
200 portion was dried under N₂ and hydrolyzed with 5% HCl in methanol at 70°C for 4 h. After cooling, an
201 appropriate volume of DCM and H₂O was added to adjust the MeOH:DCM:H₂O ratio to 1:1:0.9 (v:v:v).
202 The mixture was shaken and allowed to separate into phases, and the DCM organic phase was collected.
203 The aqueous phase was re-extracted twice with DCM. The combined organic phases were washed three
204 times with ultrapure water to remove residual acid, dried under N₂, redissolved in *n*-hexane, and filtered
205 through a 0.22 μm PTFE filter prior to analysis; the GDGTs measured in this portion correspond to total
206 extracted GDGTs. The IPL-GDGT concentration was calculated as the difference in GDGT concentration
207 between the two portions.

208 In addition, the solid residues remaining after extraction were also subjected to acid hydrolysis to
209 recover unextracted GDGTs (Huguet et al., 2010b; Tierney et al., 2012). Specifically, the solid residues
210 were first treated with dilute hydrochloric acid (HCl) to remove carbonates, then freeze-dried again.
211 Subsequently, 5 % HCl in MeOH was added, and the mixture was hydrolyzed at 70°C for 4 h. After
212 cooling, the mixture was centrifuged, and the HCl/MeOH solution was collected. The solid residue was
213 further extracted once each with DCM:MeOH (1:1, v:v) and DCM, respectively. The three extracts were
214 combined. An appropriate volume of H₂O was added to adjust the MeOH:DCM:H₂O ratio to 1:1:0.9
215 (v:v:v). After thorough mixing and phase separation, the organic phase was collected, and the aqueous
216 phase was re-extracted twice with DCM. The combined organic phases were washed three times with
217 ultrapure water to remove residual acid, dried under N₂, filtered through a 0.22 μm PTFE filter, and
218 analyzed.

219 **2.3 Calculation of GDGT Proxies**

220 The ACE salinity index, which is associated with archaeol and isoGDGTs, was calculated using the



221 formula defined by Turich and Freeman (2011) and modified by Wang et al. (2013).

$$222 \quad ACE = \frac{\text{archaeol}}{\text{archaeol} + 10 \times \text{GDGT-0}} \times 100 \quad (1)$$

223 The primary indices related to isoGDGTs include: the GDGT-0/cren ratio based on the formula
224 established by Blaga et al. (2009); the Methane Index (MI) calculated according to the formula defined
225 by Zhang et al. (2011); and the relative proportion of crenarchaeol (%cren) based on the formula defined
226 by Wang et al. (2014).

$$227 \quad MI = \frac{\text{GDGT-1} + \text{GDGT-2} + \text{GDGT-3}}{\text{GDGT-1} + \text{GDGT-2} + \text{GDGT-3} + \text{crenarchaeol} + \text{crenarchaeol}'} \quad (2)$$

$$228 \quad \%cren = \frac{\text{crenarchaeol}}{\text{GDGT-1} + \text{GDGT-2} + \text{GDGT-3} + \text{crenarchaeol} + \text{crenarchaeol}'} \quad (3)$$

229 The primary indices related to brGDGTs include: MBT' and MBT'_{SME}, calculated using the formulas
230 redefined by Peterse et al. (2014) and De Jonge et al. (2014) based on the original work of Weijers et al.
231 (2007); the IR_{6ME} index, which represents the relative abundance of 6-methyl brGDGTs versus 5-methyl
232 brGDGTs, calculated according to De Jonge et al. (2015); and the IR_{7ME} index, representing the relative
233 abundance of 7-methyl brGDGTs, calculated according to Wang et al. (2021).

$$234 \quad MBT' = \frac{Ia + Ib + Ic}{Ia + Ib + Ic + IIa + IIa' + IIb + IIb' + IIc + IIc' + IIIa + IIIa'} \quad (4)$$

$$235 \quad MBT'_{SME} = \frac{Ia + Ib + Ic}{Ia + Ib + Ic + IIa + IIb + IIc + IIIa} \quad (5)$$

$$236 \quad IR_{6ME} = \frac{IIIa' + IIIb' + IIIc' + IIa' + IIb' + IIc'}{IIIa + IIIb + IIIc + IIa + IIb + IIc + IIIa' + IIIb' + IIIc' + IIa' + IIb' + IIc'} \quad (6)$$

$$237 \quad IR_{7ME} = \frac{IIIa'' + IIIa'''}{IIIa + IIIa' + IIIa'' + IIIa''' + IIa + IIa' + IIa''} \quad (7)$$

238 The BIT index, which involves both isoGDGTs and brGDGTs, was calculated according to
239 Hopmans et al. (2004).

$$240 \quad BIT = \frac{Ia + IIa + IIIa + IIa' + IIIa'}{Ia + IIa + IIIa + IIa' + IIIa' + \text{crenarchaeol}} \quad (8)$$

241 2.4 GDGT Analysis

242 GDGTs were analyzed using HPLC-Orbitrap Exploris 120. *n*-Hexane (A) and *n*-hexane:isopropanol

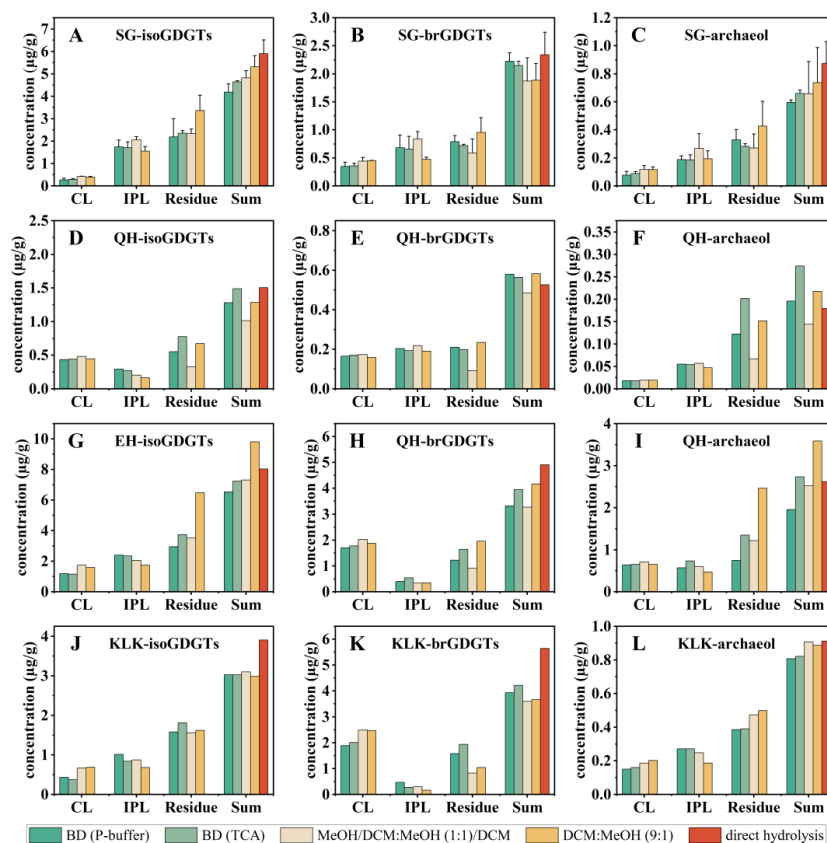


243 (9:1, v:v; B) were used as mobile phases. Isocratic elution was performed with 82 % A from 0 to 25 min,
244 followed by a linear decrease to 65 % from 25 to 50 min, and then to 0 % from 50 to 80 min, which was
245 maintained for 10 min, before finally returning to the initial conditions. The column temperature was
246 maintained at 40°C, and the mobile phase flow rate was 0.2 mL/min. The evaporator temperature was
247 set to 400°C, the ion transfer tube temperature was 300°C, and the spray current was 5 μ A. The sheath
248 gas flow rate was 30 Arb, and the auxiliary gas flow rate was 7 Arb. The resolution was set to 30,000
249 (FWHM). GDGTs and archaeol were analyzed in selected ion monitoring (SIM) mode targeting specific
250 $[M+H]^+$ ions, with the following m/z values scanned: 1302.3227, 1300.3071, 1298.2914, 1296.2757,
251 1292.2444, 1050.041, 1048.0253, 1046.0097, 1036.0253, 1034.0097, 1031.994, 1022.0097, 1019.994,
252 and 1017.9784. C_{46} GTGT was used as an internal standard for the quantification of GDGTs and archaeol
253 (Huguet et al., 2006), assuming identical response factors.

254 **3 Results**

255 **3.1 Extraction efficiencies of GDGTs for different pretreatment methods**

256 Overall, the four methods yielded high recoveries of total GDGTs in lake sediments. The GDGT
257 concentration obtained by direct acid hydrolysis was comparable to the sum of CL-GDGTs, IPL-GDGTs,
258 and residual GDGTs for each method. The minimum recoveries of isoprenoid glycerol dialkyl glycerol
259 tetraether (isoGDGTs), branched glycerol dialkyl glycerol tetraether (brGDGTs), and archaeol across
260 different methods ranged from 63.8 % to 91.9 % (Fig. 3).



261

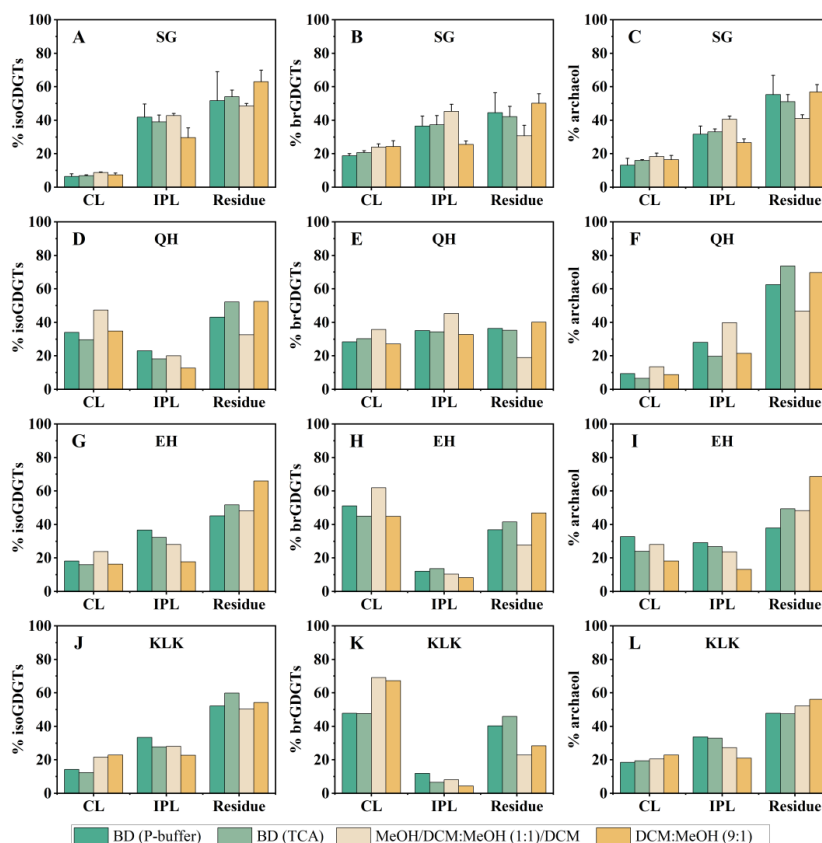
262 **Figure 3. Differences in absolute abundances of CL-GDGTs, IPL-GDGTs, and residual GDGTs extracted by**
 263 **different methods for four samples (SG: A–C; QH: D–F; EH: G–I; KLK: J–L). “Sum” represents the total of**
 264 **CL-GDGTs, IPL-GDGTs, and residual GDGTs.**

265 Abundant CL-GDGTs and IPL-GDGTs were detected in all four lake sediment samples. Compared
 266 with the two modified BD methods, the two ultrasonic extraction methods exhibited higher extraction
 267 efficiencies for CL-isoGDGTs, CL-brGDGTs, and CL-archaeol across all samples (Fig. 3), with this
 268 advantage being particularly pronounced in freshwater lake samples (EH and KLK). For the EH sample,
 269 the absolute abundances of CL-isoGDGTs and CL-brGDGTs extracted by the ultrasonic methods were
 270 approximately 500 ng/g and 200 ng/g higher, respectively, than those obtained by the BD methods (Fig.
 271 3G, H); for the KLK sample, the corresponding differences were approximately 300 ng/g and 500 ng/g,
 272 respectively (Fig. 3J, K). However, the extraction efficiencies for IPL-GDGTs varied significantly among
 273 the different methods across samples (Fig. 3). Specifically, for the SG sample, stepwise gradient
 274 extraction with MeOH, DCM:MeOH (1:1, v:v), and DCM yielded the highest extraction efficiencies for
 275 IPL-isoGDGTs, IPL-brGDGTs, and IPL-archaeol (Fig. 3A–C). In contrast, the BD (P-buffer) method
 276 achieved the highest extraction efficiencies for IPL-isoGDGTs, IPL-brGDGTs, and IPL-archaeol in the
 277 KLK sample (Fig. 3J–L). For the QH sample, the BD (P-buffer) method was most effective for extracting
 278 IPL-isoGDGTs, while the other three methods showed comparable extraction efficiencies for IPL-



279 brGDGTs and IPL-archaeol (Fig. 3D–F). For the EH sample, the BD (P-buffer) method exhibited the
280 highest extraction efficiency for IPL-isoGDGTs, whereas the BD (TCA) method performed best for IPL-
281 brGDGTs and IPL-archaeol (Fig. 3G–I). Notably, across all samples, ultrasonic extraction with
282 DCM:MeOH (9:1, v:v) yielded significantly lower extraction efficiencies for IPL-GDGTs compared to
283 the other three methods (Fig. 3).

284 To eliminate the influence of heterogeneity in total GDGT concentration among samples, the total
285 GDGTs (Sum) obtained from each pretreatment method were normalized to 100 %, and the relative
286 proportions of CL-GDGTs, IPL-GDGTs, and residual GDGTs were subsequently calculated. For the SG
287 sample, the relative proportions of IPL-isoGDGTs, IPL-brGDGTs, and IPL-archaeol were all higher than
288 those of their corresponding CL counterparts. Under the optimal extraction method, CL-isoGDGTs and
289 IPL-isoGDGTs accounted for approximately 8.8 (± 0.3) % and 42.7 (± 1.3) %, respectively; CL-brGDGTs
290 and IPL-brGDGTs accounted for approximately 24.4 (± 3.4) % and 45.3 (± 4.3) %, respectively; and CL-
291 archaeol and IPL-archaeol accounted for approximately 18.3 (± 2) % and 40.6 (± 2) %, respectively (Fig.
292 4A–C). For the QH sample, the relative proportion of IPL-isoGDGTs was lower than that of CL-
293 isoGDGTs (12.7 % and 47.4 %, respectively, under the optimal extraction method), while IPL-brGDGTs
294 and CL-brGDGTs exhibited similar proportions (45.2 % and 35.7 %, respectively, under the optimal
295 extraction method). In contrast, the proportion of IPL-archaeol was higher than that of CL-archaeol (39.8 %
296 and 13.4 %, respectively, under the optimal extraction method) (Fig. 4D–F). In the two freshwater lake
297 samples (EH and KLK), the proportions of IPL-isoGDGTs and IPL-archaeol were higher than those of
298 their corresponding CL components, whereas the proportion of IPL-brGDGTs was markedly lower than
299 that of CL-brGDGTs. For the EH sample under the optimal extraction method, the relative proportions
300 of IPL-isoGDGTs and CL-isoGDGTs were 23.8 % and 36.6 %, respectively; IPL-brGDGTs and CL-
301 brGDGTs accounted for 62 % and 13.6 %, respectively; and IPL-archaeol and CL-archaeol accounted
302 for 32.8 % and 29.2 %, respectively (Fig. 4G–I). For the KLK sample under the optimal extraction
303 method, the relative proportions of IPL-isoGDGTs and CL-isoGDGTs were 23 % and 33.4 %,
304 respectively; IPL-brGDGTs and CL-brGDGTs accounted for 69.1 % and 11.9 %, respectively; and IPL-
305 archaeol and CL-archaeol accounted for 22.8 % and 33.7 %, respectively (Fig. 4J–L).



306

307 **Figure 4. Differences in the yield of CL-GDGTs, IPL-GDGTs, and residual GDGTs extracted by different**
 308 **methods for four samples (SG: A–C; QH: D–F; EH: G–I; KLK: J–L).**

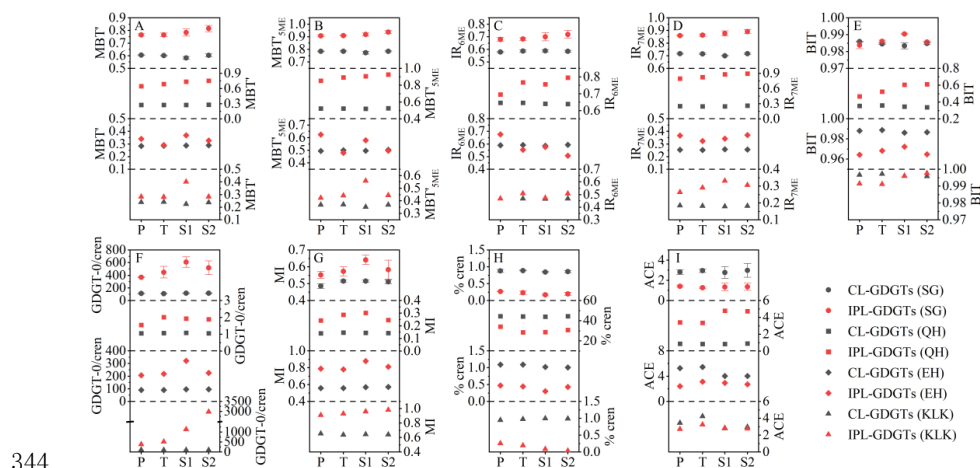
309 Furthermore, the proportion of GDGTs released by hydrolysis of the residues was relatively high
 310 across all methods. For the SG sample, the DCM:MeOH (9:1, v:v) ultrasonic extraction method yielded
 311 the highest residual GDGT proportions for isoGDGTs, brGDGTs, and archaeol, accounting for 63
 312 (± 6.9) %, 50.1 (± 5.6) %, and 56.9 (± 4.3) %, respectively (Fig. 4A–C). In contrast, stepwise gradient
 313 ultrasonic extraction with MeOH, DCM:MeOH (1:1, v:v), and DCM resulted in the lowest residual
 314 GDGT proportions for these three components, at 48.5 (± 1.6) %, 30.8 (± 6.2) %, and 41.1 (± 2.2) %, respectively (Fig. 4A–C). For the QH sample, the DCM:MeOH (9:1, v:v) ultrasonic extraction method
 316 yielded the highest residual GDGT proportions for isoGDGTs and brGDGTs, at 52.6 % and 40.2 %, respectively (Fig. 4D, F), while the BD (TCA) method yielded the highest residual proportion for archaeol at 73.7 % (Fig. 4F). The stepwise gradient ultrasonic extraction with MeOH, DCM:MeOH (1:1, v:v), and DCM yielded the lowest residual proportions for all three components, at 32.6 %, 19 %, and 46.7 %, respectively (Fig. 4D–F). For the EH sample, the DCM:MeOH (9:1, v:v) ultrasonic extraction method yielded the highest residual GDGT proportions for isoGDGTs, brGDGTs, and archaeol, at 66 %, 46.9 %, and 68.7 %, respectively (Fig. 4G–I). The BD (P-buffer) method yielded the lowest residual



323 proportions for isoGDGTs and archaeol, at 45.2 % and 38 %, respectively (Fig. 4G, I), while the stepwise
 324 gradient ultrasonic extraction with MeOH, DCM:MeOH (1:1, v:v), and DCM yielded the lowest residual
 325 proportion for brGDGTs at 27.8 % (Fig. 4H). For the KLK sample, the BD (TCA) method yielded the
 326 highest residual GDGT proportions for isoGDGTs and brGDGTs, at 59.9 % and 45.9 %, respectively
 327 (Fig. 4J, K), while the DCM:MeOH (9:1, v:v) method yielded the highest residual proportion for archaeol
 328 at 56.2 % (Fig. 4L). The stepwise gradient ultrasonic extraction with MeOH, DCM:MeOH (1:1, v:v),
 329 and DCM yielded the lowest residual proportions for isoGDGTs and brGDGTs, at 50.3 % and 22.8 %,
 330 respectively (Fig. 4J, K), whereas the BD (TCA) method yielded the lowest residual proportion for
 331 archaeol at 47.6 % (Fig. 4L).

332 3.2 Distributions of CL-GDGTs and IPL-GDGTs using different extraction methods

333 In three replicate experiments of the SG sample using different extraction methods, the standard
 334 errors for MBT', MBT'_{5ME}, IR_{6ME}, IR_{7ME}, MI, and BIT in the CL-GDGT fraction did not exceed 0.01 (Fig.
 335 5A–E, G). The maximum standard error for %cren was 0.04 (Fig. 5H), for ACE was 0.68 (Fig. 5I), and
 336 for GDGT-0/cren was 5.4 (Fig. 5F). For the IPL-GDGT fraction in the three replicate experiments of the
 337 SG sample, the maximum standard error for MBT'_{5ME} was 0.01 (Fig. 5B); for MBT', IR_{6ME}, IR_{7ME}, and
 338 BIT, the maximum standard error was 0.03 (Fig. 5A, C–E); for MI and %cren, the maximum standard
 339 error was 0.06 (Fig. 5G, H); for ACE, the maximum standard error was 0.39 (Fig. 5I); while the standard
 340 error for GDGT-0/cren was relatively large, with a maximum of 109.16 (Fig. 5F). Therefore, the
 341 systematic errors introduced by the experimental process and instrument response were minimal and
 342 negligible when comparing differences among extraction methods in this study, and replicate analysis
 343 were not performed on the other samples.



344 **Figure 5. Differences in the major indices of CL-GDGTs and IPL-GDGTs obtained using different extraction**
 345 **methods. P: BD (P-buffer) method; T: BD (TCA) method; S1: stepwise gradient extraction with MeOH,**
 346 **DCM:MeOH (1:1, v:v), and DCM; S2: DCM:MeOH (9:1, v:v).**

348 The distributions of the CL-GDGT fraction did not show significant differences among the four
 349 extraction methods, as indicated by multiple GDGT-based indices. For the four lake sediment,



350 the standard deviations of MBT', MBT'_{5ME}, IR_{6ME}, IR_{7ME}, MI, and BIT under the four extraction methods
351 were all below 0.01 (Fig. 5A–E, G); the standard deviation of GDGT-0/cren was below 3.85 (Fig. 5F);
352 the standard deviation of %cren was below 0.23 (Fig. 5H); and the standard deviation of ACE was below
353 0.78 (Fig. 5I). In contrast, the major proxies of the IPL-GDGT fraction exhibited more pronounced
354 differences among the four extraction methods. For the four lake sediment samples, the standard
355 deviations of MBT', MBT'_{5ME}, IR_{6ME}, IR_{7ME}, MI, and BIT under the four extraction methods were all
356 below 0.07 (Fig. 5A–E, G); the standard deviation of %cren was below 2.59 (Fig. 5H); and the standard
357 deviation of ACE was below 0.79 (Fig. 5I). For the SG, QH, and EH samples, the standard deviations of
358 GDGT-0/cren under the four extraction methods were all below 52.62, whereas for the KLK sample, the
359 GDGT-0/cren value obtained using the DCM:MeOH (9:1, v:v) extraction method was anomalously high,
360 differing significantly from the results of the other methods (Fig. 5F).

361 Notable differences were observed between the IPL-GDGT and CL-GDGT fractions for various
362 proxies. Under different extraction methods, the MBT', MBT'_{5ME}, IR_{6ME}, and IR_{7ME} values of the IPL-
363 GDGT fraction were higher than those of the corresponding CL-GDGT fraction in the two saline lake
364 samples (SG and QH), whereas this pattern was not evident in the two freshwater lake samples (EH and
365 KLK) (Fig. 5A–D). For the SG sample, the MBT', MBT'_{5ME}, IR_{6ME}, and IR_{7ME} values of the IPL-GDGT
366 fraction were approximately 0.18, 0.14, 0.12, and 0.16 higher, respectively, than those of the CL-GDGT
367 fraction across the four methods (Fig. 5A–D); for the QH sample, the corresponding differences were
368 approximately 0.43, 0.38, 0.11, and 0.60, respectively (Fig. 5A–D). Across all samples, the GDGT-0/cren
369 and MI values of the IPL-GDGT fraction obtained by different methods were higher than those of the
370 corresponding CL-GDGT fraction, while the %cren values were lower than those of the CL-GDGT
371 fraction (Fig. 5F–H). The BIT and ACE indices exhibited no clear patterns between the IPL-GDGT and
372 CL-GDGT fractions or among different lakes (Fig. 5E, I).

373 4 Discussion

374 4.1 Differences in recovery of CL-GDGTs and IPL-GDGTs by different methods

375 Regardless of whether assessed by absolute abundance or relative percentage, ultrasonic extraction
376 methods generally exhibited higher efficiencies for extracting CL-GDGTs from both freshwater and
377 saline lake sediments compared to the BD methods (Figs. 3 and 4), particularly for CL-isoGDGTs and
378 CL-brGDGTs in freshwater lake samples (Fig. 3G, H, J, K). Similar results have been observed in
379 previous comparative studies on GDGT extraction methods (Huguet et al., 2010b; Wang et al., 2017).
380 However, Weber et al. (2017) previously compared GDGT extraction from lake filter samples and found
381 no significant differences between the BD and ultrasonic extraction methods for CL-GDGTs. This
382 suggests that the observed extraction differences may arise not only from the affinity of GDGTs for the
383 extraction solvents but also from the environmental matrix to which GDGTs are associated or from
384 differences in their potential biological sources.

385 Notably, the extraction of IPL-GDGTs is more complex than that of CL-GDGTs. Among the
386 solvents used, MeOH:DCM (9:1) consistently yielded the lowest extraction efficiencies for IPL-GDGTs
387 across all samples (Fig. 4). For IPL-isoGDGTs in all four lake sediments, as well as for IPL-brGDGTs



388 and IPL-archaeol in the two freshwater lake sediments, the BD methods achieved the highest extraction
389 efficiencies. However, in the two saline lake sediments, stepwise gradient ultrasonic extraction with
390 MeOH, DCM:MeOH (1:1, v:v), and DCM outperformed the BD methods in extracting IPL-brGDGTs
391 and IPL-archaeol (Fig. 3B, C, E, F). Currently, knowledge regarding the biological sources and IPL
392 composition differences of living GDGTs between freshwater and saline lakes remains limited.
393 Nonetheless, notable differences exist in the composition of IPL-brGDGTs between saline and freshwater
394 lake sediments. In saline lake samples (SG and QH), the IR_{7ME} index, which represents the relative
395 abundance of ≥ 7 -methyl brGDGTs (IIIa⁺, IIa⁺) in polar lipids, was substantially higher than that in
396 freshwater lake samples (EH and KLK) (Fig. 5D). This compositional difference has also been reported
397 in global lake studies and may reflect that the producer communities of heptamethyl brGDGTs in saline
398 lakes are significantly regulated by salinity, analogous to the influence of salinity on the community
399 composition of Euryarchaeota and other archaea (Turich and Freeman, 2011; He et al., 2020; Wang et al.,
400 2021). These brGDGTs and archaeol with specific polar head groups may be more readily extracted by
401 the MeOH/DCM:MeOH (1:1)/DCM solvent combination, which may partly explain the differences in
402 IPL-brGDGT extraction efficiencies between saline and freshwater lake samples observed across
403 methods.

404 Previous comparisons of pretreatment methods using culture samples or lake filter samples revealed
405 that the BD method exhibited low recovery of highly polar IPL-GDGTs from the aqueous phase into the
406 MeOH/DCM mixed organic phase (Huguet et al., 2010b; Weber et al., 2017), with the BD (P-buffer)
407 method resulting in up to 75 % loss of IPL-brGDGTs (Weber et al., 2017). However, in the four lake
408 sediment samples of this study, the differences in brGDGT recovery between the BD methods
409 (CL+IPL+Residue) or ultrasonic extraction methods (CL+IPL+Residue) and direct acid hydrolysis were
410 not significant. Moreover, the normalized percentage abundances of each GDGT fraction were consistent
411 with the absolute abundances (Figs. 3 and 4). This indicates that GDGT loss in the aqueous phase was
412 minimal in this study, much lower than 75 %. This discrepancy may stem from the much higher
413 abundances of IPL-GDGTs representing living biomass in culture samples and SPM compared to
414 sediment samples, and may also relate to differences in the polar head groups of GDGTs within their
415 respective matrices. Although the exact reasons remain unclear, it is noteworthy that when performing
416 quantitative analysis of IPL-GDGTs, attention should be paid to the differential extraction efficiencies of
417 BD methods for different types or hydrophilic/hydrophobic IPL-GDGTs to avoid losing important GDGT
418 compositional information.

419 Compared to the potential loss of GDGTs in the aqueous phase, acid hydrolysis of the post-
420 extraction solid residues revealed that substantial amounts of GDGTs remained in the solid phase, with
421 abundances even exceeding those of CL-GDGTs or IPL-GDGTs (Figs. 3 and 4). Such GDGTs requiring
422 hydrolysis for release have been reported in lake sediment and soil samples; for instance, the proportion
423 of conventionally unextractable isoGDGTs in soil residues can reach up to 90 % (Tierney et al., 2012).
424 Similarly, Huguet et al. (2010b) noted that the majority of lipids in exponentially growing cells were not
425 effectively recovered by the tested methods, suggesting that these lipids may not originate from actively
426 dividing cells in the environment, and that approximately 70 % of IPL-GDGTs remained associated with
427 cellular material in some form, releasable only through acid hydrolysis. Furthermore, distinct differences



428 were observed among the extraction methods. Weber et al. (2017) reported for filter samples that only
429 the ultrasonic method resulted in significant loss of GDGTs to the solid residue, whereas the BD method
430 exhibited minimal solid-phase loss. In contrast, for the sediment samples in this study, both the BD and
431 ultrasonic methods resulted in relatively high proportions of GDGTs in the residues, accounting for
432 approximately 20 %–70 % of total GDGTs (Fig. 4), with the stepwise gradient method using MeOH,
433 DCM:MeOH (1:1, v:v), and DCM yielding the lowest residual GDGT amounts. Previous studies have
434 suggested that CL-GDGTs or IPL-GDGTs may not be released by conventional solvent extraction due
435 to adsorption onto soil or sediment macromolecules or mineral matrices (Tierney et al., 2012; Pei et al.,
436 2025), or because certain intact microbial cells possess “inherent recalcitrance” to organic solvent
437 extraction (Huguet et al., 2010b; Sinninghe Damsté et al., 2011, 2014; Cario et al., 2015). A recent study
438 by Pei et al. (2025) found that high-temperature pyrolysis could effectively enhance the release of bound
439 CL-GDGTs from minerals, but further extraction of IPL-GDGTs was not conducted, as high temperatures
440 may potentially affect the stability of IPL-GDGTs (Lengger et al., 2012). Therefore, further attention
441 should be directed toward the extraction methods and composition of bound IPL-GDGTs.

442 **4.2 Differences in CL-GDGT and IPL-GDGT indices under different methods**

443 Although certain differences exist in the absolute abundances of CL-GDGTs obtained by different
444 extraction methods, the indices derived from CL-isoGDGTs, CL-brGDGTs, and CL-archaeol show
445 strong consistency across methods (Fig. 5), indicating that the extraction efficiencies for different CL-
446 GDGT structures vary minimally among methods. This finding is consistent with previous method
447 comparison studies conducted on lake sediments, marine sediments, and peat, where no significant
448 differences in GDGT-based proxies were observed among extraction methods (Schouten et al., 2007;
449 Huguet et al., 2010a; Zhang et al., 2012; Wang et al., 2017). Therefore, the choice of extraction method
450 does not affect the application of CL-GDGT-based proxies in paleoclimate reconstruction and related
451 studies.

452 In contrast to CL-GDGT proxies, some IPL-GDGT-related proxies exhibit considerable variability
453 across different extraction methods. For example, the MBT'_{SME} index for the EH sample obtained by the
454 BD (P-buffer) method, and the MBT' and MBT'_{SME} indices for the KLK sample obtained by the stepwise
455 gradient method using MeOH, DCM:MeOH (1:1), and DCM, are approximately 0.1 higher than those
456 obtained by other methods. For indices such as GDGT-0/cren, where the numerator and denominator are
457 independent variables with small covariance, the differences are further amplified. For the SG sample,
458 the GDGT-0/cren index differs by up to 250 among methods, accompanied by high standard deviations
459 among replicates. For the KLK sample, the GDGT-0/cren value obtained using the DCM:MeOH (9:1)
460 method is several times higher than those obtained by other methods.

461 Two possible reasons may account for these observations. On one hand, the polarity of different
462 polar head groups varies considerably, leading to differences in their extractability; consequently, the
463 varying polarities of extraction solvents result in non-proportional extraction of different head group
464 types. On the other hand, when GDGT absolute abundances are low, as is the case for IPL-brGDGTs in
465 freshwater lakes, the variability in calculated proxy indices is further amplified. Therefore, for samples
466 with relatively low IPL-GDGT concentrations, caution should be exercised when applying the



467 subtraction method to calculate IPL-GDGT-based proxies.

468 4.3 Implications for production of GDGTs

469 Based on variations among different isoGDGT producers, several indices have been developed to
470 trace the contributions of distinct isoGDGT producers in aquatic environments, including GDGT-
471 0/crenarchaeol (Blaga et al., 2009), MI (Zhang et al., 2011), and %cren (Wang et al., 2014). Differences
472 in these indices across various environmental archives can be used to reconstruct changes in isoGDGT
473 producer communities. Multiple modern lake process studies have indicated that high GDGT-
474 0/crenarchaeol ratios or high GDGT-0 abundances are commonly observed in anoxic bottom waters,
475 suggesting that GDGT-0 is predominantly produced under anoxic conditions (Blaga et al., 2009; Baxter
476 et al., 2021). However, GDGT-0 is also abundant in anoxic sediments, with its concentration often
477 increasing with sediment depth (Tierney et al., 2012). Although the behavior of IPL-GDGTs during
478 transport and degradation from the water column to sediments is difficult to constrain precisely, the
479 higher GDGT-0 concentration and GDGT-0/crenarchaeol ratios in sediments compared to SPM appear
480 to support in situ methanogenic activity within the sediments (Blaga et al., 2009; Sinninghe Damsté et
481 al., 2009; Tierney et al., 2012; Lengger et al., 2014). In this study, the GDGT-0/cren and MI values in the
482 IPL-GDGT fraction of the four lake sediments were significantly higher than those in the CL-GDGT
483 fraction, whereas %cren in the IPL-GDGT fraction was lower than that in the CL-GDGT fraction,
484 regardless of the extracting method used (Fig. 5E–H). These findings suggest that biologically active
485 crenarchaeol is primarily produced in the lake water column rather than being newly formed in the
486 sediments, whereas GDGT-0, GDGT-1, GDGT-2, and GDGT-3 may undergo substantial in situ
487 production within the sediments or at the water-sediment interface.

488 Although the in-situ production of brGDGTs in lake water columns and sediments has been widely
489 documented (e.g., Tierney et al., 2012; Buckles et al., 2014), little attention has been paid to the in-situ
490 production of more higher methyl positional isomers of brGDGTs (IIIa", IIa"), which are predominantly
491 abundant in saline lakes (Wang et al., 2021; Kou et al., 2022). In this study, the IR_{7ME} index derived from
492 IPL-GDGTs was significantly higher than that derived from CL-GDGTs across the four lake sediments
493 (Fig. 5D), indicating the substantial presence of living or recently produced ≥ 7 -methyl brGDGTs in lake
494 sediments. Although the contributions of ≥ 7 -methyl brGDGTs produced in sediments or bottom waters
495 remain unclear, the difference in IR_{7ME} between the IPL-GDGT and CL-GDGT fractions was markedly
496 larger than those observed for MBT', MBT'_{SME}, and IR_{6ME} (Fig. 5A–D). This suggests that ≥ 7 -methyl
497 brGDGTs may be produced in larger quantities compared with other brGDGTs within sediments (or at
498 the water-sediment interface), or alternatively, they may be generated in deeper water layers and degrade
499 more slowly compared to other brGDGTs. Furthermore, in the two saline lake sediment samples, the
500 MBT', MBT'_{SME}, IR_{6ME}, and IR_{7ME} indices derived from IPL-GDGTs were consistently higher than those
501 derived from CL-GDGTs (Fig. 5A–D). This may imply that bacteria producing 7-methyl brGDGTs may
502 also synthesize other types of brGDGTs. A previous global lake survey by Wang et al. (2021) indicated
503 that the relative abundance of 7-methyl brGDGTs is strongly regulated by salinity, and that MBT'_{SME} is
504 influenced by salinity-driven isomerization of brGDGTs. This is consistent with the observations in this
505 study, where producers of 7-methyl brGDGTs may simultaneously produce tetramethylated brGDGTs



506 (Ia, Ib and Ic), leading to coordinated variations in the MBT¹ and MBT^{5ME} indices and consequently
507 introducing bias into temperature proxies.

508 **5 Conclusions**

509 In this study, by comparing the performance of two modified Bligh-Dyer methods and two
510 ultrasonic extraction methods for GDGT extraction in sediment samples from two saline lakes and two
511 freshwater lakes, we found that stepwise gradient ultrasonic extraction with MeOH, DCM:MeOH (1:1,
512 v:v), and DCM generally yielded the highest extraction efficiency for CL-GDGTs. However, the major
513 indices derived from CL-GDGTs showed no significant differences among the different extraction
514 methods, indicating that extraction methods do not affect the calculation of these proxies in paleoclimate
515 reconstruction. In contrast, the extraction results for IPL-GDGTs varied considerably, with differences
516 observed across methods, lake salinity regimes (saline vs. freshwater), and GDGT components
517 (isoGDGTs, brGDGTs, and archaeol). Therefore, when quantifying IPL-GDGTs, it is recommended to
518 select an appropriate extraction method through preliminary comparative experiments. Furthermore, a
519 substantial proportion of GDGTs may be occluded within sediments and cannot be fully extracted by
520 conventional solvents.

521 Comparisons of distributional differences between CL-GDGT and IPL-GDGT fractions further
522 revealed that crenarchaeol is primarily produced in the lake water column, whereas GDGT-0, GDGT-1,
523 GDGT-2, and GDGT-3 undergo significant in-situ production in sediments or at the water-sediment
524 interface. In saline environments, ≥7-methyl brGDGTs might also be abundantly produced in sediments
525 or at the water-sediment interface, and their source bacteria are likely to also synthesize tetramethylated
526 brGDGTs, thereby affecting the interpretation and application of the relevant methylation indices.

527 **Data availability**

528 The data used for this study can be found in the supplement.

529

530

531 **Author contributions**

532 HW conceptualized the study, supervised the project and secured funding; RM conducted the
533 experiments, analyzed the data and wrote the manuscript draft; RM, NS, ZZ, HL, and XL developed the
534 methodology; HW reviewed and edited the manuscript.



535 **Competing interests**

536 The contact author has declared that none of the authors has any competing interests.

537 **Disclaimer**

538 The authors declare that this work has not been published nor is under consideration anywhere else.

539 **Acknowledgments**

540 We thank Weiguo Liu, Xijin Cao, and Taibei Liu for help in field sampling.

541 **Financial support**

542 This research was financially supported by the National Natural Science Foundation of China (Grant No.

543 42273030) and National Key Research and Development Program of China (2023YFF0804300).

544 **References**

- 545 Baxter, A. J., van Bree, L. G. J., Peterse, F., Hopmans, E. C., Villanueva, L., Verschuren, D., and
546 Sinninghe Damsté, J. S.: Seasonal and multi-annual variation in the abundance of isoprenoid GDGT
547 membrane lipids and their producers in the water column of a meromictic equatorial crater lake (Lake
548 Chala, East Africa), *Quat. Sci. Rev.*, 273, 107263, <https://doi.org/10.1016/j.quascirev.2021.107263>, 2021.
- 549 Bijl, P. K., Sliwinska, K. K., Duncan, B., Huguet, A., Naeher, S., Rattanasriampaipong, R., de Oca, C. S.
550 M., Auderset, A., Berke, M. A., Kim, B. S., Davtian, N., Jones, T. D., Eefting, D. D., Elling, F. J., Fenies,
551 P., Inglis, G. N., O'Connor, L., Pancost, R. D., Peterse, F., Rice, A., Sluijs, A., Varma, D., Xiao, W. J.,
552 and Zhang, Y. G.: Reviews and syntheses: Best practices for the application of marine GDGTs as proxy
553 for paleotemperatures: sampling, processing, analyses, interpretation, and archiving protocols,
554 *Biogeosciences*, 22, 6465-6508, <https://doi.org/10.5194/bg-22-6465-2025>, 2025.
- 555 Blaga, C. I., Reichert, G. J., Heiri, O., and Sinninghe Damsté, J. S.: Tetraether membrane lipid
556 distributions in water-column particulate matter and sediments: a study of 47 European lakes along a
557 north-south transect, *J. Paleolimnol.*, 41, 523-540, <https://doi.org/10.1007/s10933-008-9242-2>, 2009.
- 558 Bligh, E. G., and Dyer, W. J.: A rapid method of total lipid extraction and purification. *Can. J. Biochem,*
559 *Physiol.*, 37, 911-917, <https://doi.org/10.1139/o59-099>, 1959.
- 560 Buckles, L. K., Weijers, J. W. H., Verschuren, D., and Sinninghe Damsté, J. S.: Sources of core and intact
561 branched tetraether membrane lipids in the lacustrine environment: Anatomy of Lake Challa and its



562 catchment, equatorial East Africa, *Geochim. Cosmochim. Acta*, 140, 106-126,
563 <https://doi.org/10.1016/j.gca.2014.04.042>, 2014.

564 Cario, A., Grossi, V., Schaeffer, P., and Oger, P. M.: Membrane homeoviscous adaptation in the piezo-
565 hyperthermophilic archaeon *Thermococcus barophilus*, *Front. Microbiol.*, 6, 1152,
566 <https://doi.org/10.3389/fmicb.2015.01152>, 2015.

567 Chen, Y., Zhang, C., Jia, C., Zheng, F., and Zhu, C.: Tracking the signals of living archaea: A multiple
568 reaction monitoring (MRM) method for detection of trace amounts of intact polar lipids from the natural
569 environment, *Org. Geochem.*, 97, 1-4, <https://doi.org/10.1016/j.orggeochem.2016.04.006>, 2016.

570 De Jonge, C., Hopmans, E. C., Zell, C. I., Kim, J. H., Schouten, S., and Sinninghe Damsté, J. S.:
571 Occurrence and abundance of 6-methyl branched glycerol dialkyl glycerol tetraethers in soils:
572 Implications for palaeoclimate reconstruction, *Geochim. Cosmochim. Acta*, 141, 97-112,
573 <https://doi.org/10.1016/j.gca.2014.06.013>, 2014.

574 De Jonge, C., Stadnitskaia, A., Fedotov, A., and Sinninghe Damsté, J. S.: Impact of riverine suspended
575 particulate matter on the branched glycerol dialkyl glycerol tetraether composition of lakes: The outflow
576 of the Selenga River in Lake Baikal (Russia), *Org. Geochem.*, 83-84, 241-252,
577 <https://doi.org/10.1016/j.orggeochem.2015.04.004>, 2015.

578 Escala, M., Rosell-Melé, A., and Masqué, P.: Rapid screening of glycerol dialkyl glycerol tetraethers in
579 continental Eurasia samples using HPLC/APCI-ion trap mass spectrometry, *Org. Geochem.*, 38, 161-164,
580 <https://doi.org/10.1016/j.orggeochem.2006.08.013>, 2007.

581 Evans, T. W., Elling, F. J., Li, Y. L., Pearson, A., and Summons, R. E.: A new and improved protocol for
582 extraction of intact polar membrane lipids from archaea, *Org. Geochem.*, 165, 104353,
583 <https://doi.org/10.1016/j.orggeochem.2021.104353>, 2022.

584 Hopmans, E. C., Weijers, J. W. H., Schefuß, E., Herfort, L., Sinninghe Damsté, J. S., and Schouten, S.:
585 A novel proxy for terrestrial organic matter in sediments based on branched and isoprenoid tetraether
586 lipids, *Earth Planet. Sci. Lett.*, 224, 107-116. <https://doi.org/10.1016/j.epsl.2004.05.012>, 2004.

587 Horai, S., Yamauchi, N., and Naraoka, H.: Simultaneous total analysis of core and polar membrane lipids
588 in archaea by high-performance liquid chromatography/high-resolution mass spectrometry coupled with
589 heated electrospray ionization, *Rapid Commun. Mass Spectrom.*, 33, 1571-1577,



- 590 <https://doi.org/10.1002/rcm.8506>, 2019.
- 591 Huguet, A., Fosse, C., Laggoun-Défarge, F., Toussaint, M.-L., and Derenne, S.: Occurrence and
592 distribution of glycerol dialkyl glycerol tetraethers in a French peat bog, *Org. Geochem.*, 41, 559-572,
593 <https://doi.org/10.1016/j.orggeochem.2010.02.015>, 2010a.
- 594 Huguet, C., Hopmans, E. C., Febo-Ayala, W., Thompson, D. H., Sinninghe Damsté, J. S., and Schouten,
595 S.: An improved method to determine the absolute abundance of glycerol dibiphytanyl glycerol tetraether
596 lipids, *Org. Geochem.*, 37, 1036-1041, <https://doi.org/10.1016/j.orggeochem.2006.05.008>, 2006.
- 597 Huguet, C., Martens-Habbena, W., Urakawa, H., Stahl, D. A., and Ingalls, A. E.: Comparison of
598 extraction methods for quantitative analysis of core and intact polar glycerol dialkyl glycerol tetraethers
599 (GDGTs) in environmental samples, *Limnol. Oceanogr.: Methods*, 8, 127-145,
600 <https://doi.org/10.4319/lom.2010.8.127>, 2010b.
- 601 Ingalls, A. E., Huguet, C., and Truxal, L. T.: Distribution of Intact and Core Membrane Lipids of Archaeal
602 Glycerol Dialkyl Glycerol Tetraethers among Size-Fractionated Particulate Organic Matter in Hood
603 Canal, Puget Sound, *Appl. Environ. Microbiol.*, 78, 1480-1490, <https://doi.org/10.1128/AEM.07016-11>,
604 2012.
- 605 Inglis, G. N., Bhattacharya, T., Hemingway, J. D., Hollingsworth, E. H., Feakins, S. J., and Tierney, J. E.:
606 Biomarker Approaches for Reconstructing Terrestrial Environmental Change, *Annu. Rev. Earth and*
607 *Planet. Sci.*, 50, 369-394, <https://doi.org/10.1146/annurev-earth-032320-095943>, 2022.
- 608 Kou, Q. Q., Zhu, L. P., Ju, J. T., Wang, J. B., Xu, T., Li, C. L., and Ma, Q. F.: Influence of salinity on
609 glycerol dialkyl glycerol tetraether-based indicators in Tibetan Plateau lakes: Implications for
610 paleotemperature and paleosalinity reconstructions, *Palaeogeogr. Palaeoclimatol. Palaeoecol.*, 601,
611 111127, <https://doi.org/10.1016/j.palaeo.2022.111127>, 2022.
- 612 Lanzhou Institute of Geology, Institute of hydrobiology, Institute of Microbiology, and Nanjing Institute
613 of Geology and Paleontology, Chinese Academy of Sciences: Comprehensive investigation report on
614 Qinghai Lake, Science Press, Beijing (in Chinese), 1979.
- 615 Lengger, S. K., Hopmans, E. C., Sinninghe Damsté, J. S., and Schouten, S.: Comparison of extraction
616 and work up techniques for analysis of core and intact polar tetraether lipids from sedimentary
617 environments, *Org. Geochem.*, 47, 34-40, <https://doi.org/10.1016/j.orggeochem.2012.02.009>, 2012.



618 Lengger, S. K., Hopmans, E. C., Sinninghe Damsté, J. S., and Schouten, S.: Impact of sedimentary
619 degradation and deep water column production on GDGT abundance and distribution in surface
620 sediments in the Arabian Sea: Implications for the TEX₈₆ paleothermometer, *Geochim. Cosmochim. Acta*,
621 142, 386-399, <https://doi.org/10.1016/j.gca.2014.07.013>, 2014.

622 Li, T., Luo, Y., Liu, C., Lu, X., and Feng, B.: Archaeal Lipids: Extraction, Separation, and Identification
623 via Natural Product Chemistry Perspective, *Int. J. Mol. Sci.*, 26, 3167,
624 <https://doi.org/10.3390/ijms26073167>, 2025.

625 Meegan Kumar, D., Woltering, M., Hopmans, E. C., Sinninghe Damsté, J. S., Schouten, S., and Werne,
626 J. P.: The vertical distribution of Thaumarchaeota in the water column of Lake Malawi inferred from core
627 and intact polar tetraether lipids, *Org. Geochem.*, 132, 37-49,
628 <https://doi.org/10.1016/j.orggeochem.2019.03.004>, 2019.

629 Nishihara, M., and Koga, Y.: Extraction and Composition of Polar Lipids from the Archaeobacterium,
630 *Methanobacterium thermoautotrophicum*: Effective Extraction of Tetraether Lipids by an Acidified
631 Solvent, *J. Biochem.*, 101, 997-1005, <https://doi.org/10.1093/oxfordjournals.jbchem.a121969>, 1987.

632 Pearson, E. J., Juggins, S., Talbot, H. M., Weckström, J., Rosén, P., Ryves, D. B., Roberts, S. J., and
633 Schmidt, R.: A lacustrine GDGT-temperature calibration from the Scandinavian Arctic to Antarctic:
634 Renewed potential for the application of GDGT-paleothermometry in lakes, *Geochim. Cosmochim. Acta*,
635 75, 6225-6238, <https://doi.org/10.1016/j.gca.2011.07.042>, 2011.

636 Pei, H., Yang, H., Kuzyakov, Y., Luo, G., Dang, X., and Xie, S.: Mineral-bound lipid formation in soils
637 and sediments: the importance of microbial pathways, *Soil Biol. Biochem.*, 209, 109883,
638 <https://doi.org/10.1016/j.soilbio.2025.109883>, 2025.

639 Peterse, F., Vonk, J. E., Holmes, R. M., Giosan, L., Zimov, N., and Eglinton, T. I.: Branched glycerol
640 dialkyl glycerol tetraethers in Arctic lake sediments: Sources and implications for paleothermometry at
641 high latitudes, *J. Geophys. Res. Biogeosci.*, 119, 1738-1754, <https://doi.org/10.1002/2014JG002639>,
642 2014.

643 Pitcher, A., Hopmans, E. C., Mosier, A. C., Park, S. J., Rhee, S. K., Francis, C. A., Schouten, S., and
644 Sinninghe Damsté, J. S.: Core and Intact Polar Glycerol Dibiphytanyl Glycerol Tetraether Lipids of
645 Ammonia-Oxidizing Archaea Enriched from Marine and Estuarine Sediments, *Appl. Environ. Microbiol.*,



- 646 77, 3468-3477, <https://doi.org/10.1128/AEM.02758-10>, 2011.
- 647 Pitcher, A., Hopmans, E. C., Schouten, S., and Sinninghe Damsté, J. S.: Separation of core and intact
648 polar archaeal tetraether lipids using silica columns: Insights into living and fossil biomass contributions,
649 *Org. Geochem.*, 40, 12-19, <https://doi.org/10.1016/j.orggeochem.2008.09.008>, 2009.
- 650 Qian, S., Yang, H., Dong, C., Wang, Y., Wu, J., Pei, H., Dang, X., Lu, J., Zhao, S., and Xie, S.: Rapid
651 response of fossil tetraether lipids in lake sediments to seasonal environmental variables in a shallow
652 lake in central China: Implications for the use of tetraether-based proxies, *Org. Geochem.*, 128, 108-121,
653 <https://doi.org/10.1016/j.orggeochem.2018.12.007>, 2019.
- 654 Raberg, J. H., Flores, E., Crump, S. E., de Wet, G., Dildar, N., Miller, G. H., Geirsdóttir, Á., and
655 Sepúlveda, J.: Intact Polar brGDGTs in Arctic Lake Catchments: Implications for Lipid Sources and
656 Paleoclimate Applications, *J. Geophys. Res. Biogeosci.*, 127, e2022JG006969,
657 <https://doi.org/10.1029/2022JG006969>, 2022.
- 658 Rezanka, T., Kyselová, L., and Murphy, D. J.: Archaeal lipids, *Prog. Lipid Res.*, 91, 101237,
659 <https://doi.org/10.1016/j.plipres.2023.101237>, 2023.
- 660 Schouten, S., Hopmans, E. C., Baas, M., Boumann, H., Standfest, S., Könneke, M., Stahl, D. A., and
661 Sinninghe Damsté, J. S.: Intact Membrane Lipids of “*Candidatus Nitrosopumilus maritimus*,” a
662 Cultivated Representative of the Cosmopolitan Mesophilic Group I Crenarchaeota, *Appl. Environ.*
663 *Microbiol.*, 74, 2433-2440, <https://doi.org/10.1128/aem.01709-07>, 2008.
- 664 Schouten, S., Hopmans, E. C., and Sinninghe Damsté, J. S.: The organic geochemistry of glycerol dialkyl
665 glycerol tetraether lipids: A review, *Org. Geochem.*, 54, 19-61,
666 <https://doi.org/10.1016/j.orggeochem.2012.09.006>, 2013.
- 667 Schouten, S., Hugué, C., Hopmans, E. C., Kienhuis, M. V. M., and Sinninghe Damsté, J. S.: Analytical
668 methodology for TEX₈₆ paleothermometry by high-performance liquid chromatography/atmospheric
669 pressure chemical ionization-mass spectrometry, *Anal. Chem.*, 79, 2940-2944,
670 <https://doi.org/10.1021/ac062339v>, 2007.
- 671 Sinninghe Damsté, J. S., Ossebaar, J., Abbas, B., Schouten, S., and Verschuren, D.: Fluxes and
672 distribution of tetraether lipids in an equatorial African lake: Constraints on the application of the TEX₈₆
673 palaeothermometer and BIT index in lacustrine settings, *Geochim. Cosmochim. Acta*, 73, 4232-4249,



- 674 <https://doi.org/10.1016/j.gca.2009.04.022>, 2009.
- 675 Sinninghe Damsté, J. S., Rijpstra, W. I. C., Hopmans, E. C., Weijers, J. W. H., Foesel, B. U., Overmann,
676 J., and Dedysh, S.N.: 13,16-Dimethyl Octacosanedioic Acid (iso-Diabolic Acid), a Common Membrane-
677 Spanning Lipid of Acidobacteria Subdivisions 1 and 3, *Appl. Environ. Microbiol.*, *77*, 4147-4154,
678 <https://doi.org/10.1128/aem.00466-11>, 2011.
- 679 Sinninghe Damsté, J. S., Rijpstra, W. I. C., Hopmans, E. C., Foesel, B. U., Wüst, P. K., Overmann, J.,
680 Tank, M., Bryant, D. A., Dunfield, P. F., Houghton, K., and Stott, M. B.: Ether- and Ester-Bound iso-
681 Diabolic Acid and Other Lipids in Members of Acidobacteria Subdivision 4, *Appl. Environ. Microbiol.*,
682 *80*, 5207-5218, <https://doi.org/10.1128/AEM.01066-14>, 2014.
- 683 Sturt, H. F., Summons, R. E., Smith, K., Elvert, M., and Hinrichs, K.-U.: Intact polar membrane lipids in
684 prokaryotes and sediments deciphered by high-performance liquid chromatography/electrospray
685 ionization multistage mass spectrometry-new biomarkers for biogeochemistry and microbial ecology,
686 *Rapid Commun. Mass Spectrom.*, *18*, 617-628, <https://doi.org/10.1002/rcm.1378>, 2004.
- 687 Tierney, J. E., Schouten, S., Pitcher, A., Hopmans, E. C., and Sinninghe Damsté, J. S.: Core and intact
688 polar glycerol dialkyl glycerol tetraethers (GDGTs) in Sand Pond, Warwick, Rhode Island (USA):
689 Insights into the origin of lacustrine GDGTs, *Geochim. Cosmochim. Acta*, *77*, 561-581,
690 <https://doi.org/10.1016/j.gca.2011.10.018>, 2012.
- 691 Turich, C., and Freeman, K. H.: Archaeal lipids record paleosalinity in hypersaline systems, *Org.*
692 *Geochem.*, *42*, 1147-1157, <https://doi.org/10.1016/j.orggeochem.2011.06.002>, 2011.
- 693 van Bree, L. G. J., Peterse, F., Baxter, A. J., De Crop, W., van Grinsven, S., Villanueva, L., Verschuren,
694 D., and Sinninghe Damsté, J. S.: Seasonal variability and sources of in situ brGDGT production in a
695 permanently stratified African crater lake, *Biogeosciences*, *17*, 5443-5463, [https://doi.org/10.5194/bg-](https://doi.org/10.5194/bg-17-5443-2020)
696 [17-5443-2020](https://doi.org/10.5194/bg-17-5443-2020), 2020.
- 697 van Mooy, B. A. S., and Fredricks, H. F.: Bacterial and eukaryotic intact polar lipids in the eastern
698 subtropical South Pacific: Water-column distribution, planktonic sources, and fatty acid composition,
699 *Geochim. Cosmochim. Acta*, *74*, 6499-6516, <https://doi.org/10.1016/j.gca.2010.08.026>, 2010.
- 700 Wang, H., Dong, H., Zhang, C., Jiang, H., Zhao, M., Liu, Z., Lai, Z., and Liu, W.: Water depth affecting
701 thaumarchaeol production in Lake Qinghai, northeastern Qinghai-Tibetan plateau: Implications for paleo



- 702 lake levels and paleoclimate, *Chem. Geol.*, 368, 76-84, <https://doi.org/10.1016/j.chemgeo.2014.01.009>,
703 2014.
- 704 Wang, H., Liu, W., He, Y., Zhou, A., Zhao, H., Liu, H., Cao, Y., Hu, J., Meng, B., Jiang, J., Kolpakova,
705 M., Krivonogov, S., and Liu, Z.: Salinity-controlled isomerization of lacustrine brGDGTs impacts the
706 associated MBT_{SME} terrestrial temperature index, *Geochim. Cosmochim. Acta*, 305, 33-48,
707 <https://doi.org/10.1016/j.gca.2021.05.004>, 2021.
- 708 Wang, H., Liu, W., Zhang, C., Jiang, H., Dong, H., Lu, H., and Wang, J.: Assessing the ratio of archaeol
709 to caldarchaeol as a salinity proxy in highland lakes on the northeastern Qinghai–Tibetan Plateau, *Org.*
710 *Geochem*, 54, 69-77, <https://doi.org/10.1016/j.orggeochem.2012.09.011>, 2013.
- 711 Wang, H., Liu, W., and Zhang, C.: Comparison of the ultrasound-assisted organic solvent extraction and
712 modified Bligh-Dyer extraction for the analysis of glycerol dialkyl glycerol tetraethers from
713 environmental samples, *J. Earth Environ. Sci.*, 8, 176-184, <http://dx.doi.org/10.7515/JEE201702010>, 2017.
- 714 Weber, Y., Sinninghe Damsté, J. S., Zopfi, J., De Jonge, C., Gilli, A., Schubert, C. J., Lepori, F., Lehmann,
715 M. F., and Niemann, H.: Redox-dependent niche differentiation provides evidence for multiple bacterial
716 sources of glycerol tetraether lipids in lakes, *Proc. Natl. Acad. Sci. USA*, 115, 10926-10931,
717 <https://doi.org/10.1073/pnas.1805186115>, 2018.
- 718 Weber, Y., Sinninghe Damsté, J. S., Hopmans, E. C., Lehmann, M. F., and Niemann, H.: Incomplete
719 recovery of intact polar glycerol dialkyl glycerol tetraethers from lacustrine suspended biomass, *Limnol.*
720 *Oceanogr.: Methods*, 15, 782-793, <https://doi.org/10.1002/lom3.10198>, 2017.
- 721 Weijers, J. W. H., Schouten, S., van den Donker, J. C., Hopmans, E. C., and Sinninghe Damsté, J. S.:
722 Environmental controls on bacterial tetraether membrane lipid distribution in soils, *Geochim.*
723 *Cosmochim. Acta*, 71, 703-713, <https://doi.org/10.1016/j.gca.2006.10.003>, 2007.
- 724 White, D. C., Davis, W. M., Nickels, J. S., King, J. D., and Bobbie, R. J.: Determination of the
725 sedimentary microbial biomass by extractable lipid phosphate, *Oecologia*, 40, 51-62,
726 <https://doi.org/10.1007/BF00388810>, 1979.
- 727 Wang, S. M., and Dou, H. S.: *Lake in China*. Science Press, Beijing (In Chinese), 1998.
- 728 Zhang, C., Wang, J., Wei, Y., Zhu, C., Huang, L., and Dong, H.: Production of Branched Tetraether Lipids
729 in the Lower Pearl River and Estuary: Effects of Extraction Methods and Impact on bGDGT Proxies,



- 730 Front. Microbio., 2, 274, <https://doi.org/10.3389/fmicb.2011.00274>, 2012.
- 731 Zhang, Y. G., Zhang, C. L., Liu, X.-L., Li, L., Hinrichs, K.-U., and Noakes, J. E.: Methane Index: A
732 tetraether archaeal lipid biomarker indicator for detecting the instability of marine gas hydrates, Earth
733 Planet. Sci. Lett., 307, 525-534, <https://doi.org/10.1016/j.epsl.2011.05.031>, 2011.
- 734 Zheng, F., Yao, W., He, W., Zhang, W., Chen, Y., Chen, H., Zeng, Z., Liu, X.-L., Ding, S., Zheng, Y.,
735 Huang, L., Zhu, Y., and Zhang, C.: A comprehensive database for high-throughput identification of
736 archaeal lipids using high-resolution mass spectrometry, Nat. Commun., 17, 588,
737 <https://doi.org/10.1038/s41467-025-67286-3>, 2025.
- 738 Zhu, C., Lipp, J. S., Wörmer, L., Becker, K. W., Schröder, J., and Hinrichs, K.-U.: Comprehensive
739 glycerol ether lipid fingerprints through a novel reversed phase liquid chromatography–mass
740 spectrometry protocol, Org. Geochem., 65, 53-62, <https://doi.org/10.1016/j.orggeochem.2013.09.012>,
741 2013.
- 742 Zink, K.-G., Mangelsdorf, K., Granina, L., and Horsfield, B.: Estimation of bacterial biomass in
743 subsurface sediments by quantifying intact membrane phospholipids, Anal. Bioanal. Chem., 390, 885-
744 896, <https://doi.org/10.1007/s00216-007-1732-y>, 2008.